Atmos. Chem. Phys. Discuss., 6, 3403–3417, 2006
www.atmos-chem-phys-discuss.net/6/3403/2006/

Atmospheric Chemistry and Physics Discussions

Persistence and photochemical decay of springtime total ozone anomalies in the Canadian Middle Atmosphere Model

S. Tegtmeier[1,2] **and T. G. Shepherd**[2]

[1]Alfred Wegener Institute for Polar and Marine Research, Potsdam, Germany
[2]Department of Physics, University of Toronto, Toronto, Ontario, Canada

Received: 19 January 2006 – Accepted: 10 February 2006 – Published: 28 April 2006

Correspondence to: S. Tegtmeier (stegtmeier@awi-potsdam.de)

Abstract

The persistence and decay of springtime total ozone anomalies over the entire extratropics (midlatitudes plus polar regions) is analysed using results from the Canadian Middle Atmosphere Model (CMAM), a comprehensive chemistry-climate model. As in the observations, interannual anomalies established through winter and spring persist with very high correlation coefficients (above 0.8) through summer until early autumn, while decaying in amplitude as a result of photochemical relaxation in the quiescent summertime stratosphere. The persistence and decay of the ozone anomalies in CMAM agrees extremely well with observations, even in the southern hemisphere when the model is run without heterogeneous chemistry (in which case there is no ozone hole and the seasonal cycle of ozone is quite different from observations), and even in the northern hemisphere where this version of CMAM (run with fixed external forcing) strongly underestimates the observed interannual variability. This shows that ozone anomaly persistence and decay does not depend on how the springtime anomalies are created or on their magnitude, but reflects the transport and photochemical decay in the model. It is thus a robust diagnostic of model performance.

1 Introduction

Fioletov and Shepherd (2003, hereinafter referred to as F&S 2003) showed that interannual total ozone anomalies in midlatitudes develop through the winter and spring, and then persist through summer until autumn. Weber et al. (2003) showed that these anomalies (in both spring and late summer) are related to anomalies in the dynamical forcing of the Brewer-Dobson circulation. During winter and early spring there is a buildup of ozone which is caused by the dominance of transport processes during this period. This buildup is followed by a decline through late spring and summer when transport becomes less important and photochemical loss controls the time evolution of midlatitude total ozone. During this summertime period of total ozone decline the

ACPD

6, 3403–3417, 2006

ozone anomalies decrease in magnitude through photochemical relaxation, and then are rapidly erased when the next winter's buildup begins. In general the persistence of the midlatitude ozone anomalies is stronger in the northern hemisphere (NH) than in the southern hemisphere (SH). This is due to the influence of springtime polar ozone depletion on midlatitude ozone after the breakup of the vortex. Fioletov and Shepherd (2005, hereinafter referred to as F&S 2005) went on to show that the persistence of the total ozone anomalies is much greater in the SH when the entire extratropics (35° S–80° S) is included, since the region is then not sensitive to transport across 60° S. (The region poleward of 80° latitude is not observed by TOMS or SBUV, but because of the very small area involved contributes very little to the entire extratropical amounts.)

These observed relationships provide a valuable diagnostic for process-oriented model validation. The F&S 2003 approach is used here to compare the persistence and photochemical decay of total ozone anomalies in the Canadian Middle Atmosphere Model (CMAM) with observations.

2 Data sets and methodology

We use the same version of the merged satellite data set as in F&S 2005. The set is prepared by NASA and combines version 8 of the TOMS and SBUV data for the time period from November 1978 to December 2003 (Frith et al., 2004). The zonal mean total ozone values cover up to 80° N from April to September in the NH and up to 80° S from October to March in the SH. The data for August and September 1995 as well as May and June 1996 are missing. We use estimates of total ozone from ground based measurements to fill the gaps (Fioletov et al., 2002). The 24-year time series of each month consists of monthly and zonal means which are area weighted and averaged over certain latitude bands. As in F&S 2005 we use the equivalent effective stratospheric chlorine (EESC) (WMO, 2003) as a proxy for the long term trend of each time series, and remove the EESC fit prior to the anomaly analysis.

The CMAM is a three-dimensional chemistry-climate model with comprehensive

ACPD
6, 3403–3417, 2006

physical parameterisations (Beagley et al., 1997; de Grandpré et al., 2000). The version used here has a domain from the surface of the earth to approximately 97 km and T32 spectral truncation. The model includes a fully interactive stratospheric chemistry with all the relevant catalytic ozone loss cycles and heterogeneous reactions for sulphate aerosols, liquid ternary solutions (the so-called Type 1b Polar Stratospheric Clouds, PSCs) and water ice (Type 2 PSCs). There is no parameterisation of nitric acid trihydrate PSCs (Type 1a PSCs) or any associated denitrification. To calculate the persistence and photochemical decay of total ozone anomalies in CMAM we use ozone data from a 20-year run of the model performed under fixed external forcings corresponding to conditions in 2000, with annually repeating climatological sea surface temperatures.

The total ozone autocorrelations were calculated for the entire extratropics for both hemispheres (35°–80° latitude) as a function of time lag for each month of the year. The autocorrelation is thus

$$R(t,\tau) = \frac{\sum_{i=1}^{n} f_i(t) f_i(t+\tau)}{\sqrt{\sum_{i=1}^{n} f_i(t)^2}\sqrt{\sum_{i=1}^{n} f_i(t+\tau)^2}}$$

where n is the number of years in the record, t is a particular month, $t+\tau$ is a subsequent month lagged by τ months, and f_i is the deviation from the mean in the year i. The correlation coefficients between ozone values for the same month in different years are low. Thus each year can be considered as independent and correlation coefficients greater than 0.4 are statistically significant at the 95% confidence level.

3 Results

Figure 1 shows the seasonal cycle of total ozone in the SH from both observations and from CMAM, averaged over 35° S–60° S, 60° S–80° S and 35° S–80° S for each year in the relevant data sets. The observed values are the anomalies from the long

ACPD
6, 3403–3417, 2006

term trend added to the EESC fit for the year 2000. In this way, the absolute values are directly comparable to those of the CMAM which represent year 2000 conditions. The seasonal cycle of total ozone shows a late spring maximum in midlatitudes and a late spring minimum in polar regions, the latter reflecting the springtime polar ozone depletion. CMAM midlatitude ozone levels exhibit a high bias of between 10 and 20 DU relative to observations. Furthermore, the seasonal cycle of total ozone for the entire extratropical region is relatively flat in CMAM.

As noted in F&S 2003, the anomalies established in spring appear to persist through the summer. This is illustrated by Fig. 2, which shows the year to year variability of total ozone averaged over the SH extratropics for the four spring/early summer months for both observations (normalized to the year 2000) and model. The interannual anomalies are highly correlated from month to month, and the anomalies established in October decrease continuously through January. Since the seasonal cycle of the CMAM ozone is relatively flat the overall absolute decrease in ozone values during the four months is smaller in CMAM than in the observations, but the magnitude of the year to year variability of each month is in reasonably good agreement between the two data sets.

Figure 3 shows the correlation coefficients between ozone values at a given month of the year with ozone values at subsequent months for the SH extratropics. Colours denote statistically significant correlations at the 95% confidence level assuming each year is independent. The correlations are extremely high (above 0.8) in summer (November until February) with any later month up to March, and statistically significant up to April. Thus, it is evident that the anomalies persist from the end of spring until early autumn in both observations and the CMAM. This high predictability of total ozone reflects the fact that there is not a great deal of dynamical variability in the summer stratosphere, and so the time evolution of ozone (integrated over the extratropics) is controlled by photochemical relaxation.

The relationship between ozone anomalies in November and in subsequent months can be estimated by linear regression, and is shown in Fig. 4. The regression coefficients illustrate that the amplitude of the ozone anomalies decays on a timescale of a

few months through photochemical ozone loss. Again the CMAM results are very similar to the observations, indicating that the overall summertime ozone photochemistry in the model is reasonable.

Figure 4 also shows results from a different version of CMAM which includes no heterogeneous chemistry and thus has no ozone hole. (Two 15-year simulations were used to obtain a combined 30-year ozone data set.) The seasonal cycle of total ozone for this simulation is very different, as seen in Fig. 5 (which is to be compared with Fig. 1). Since there is no springtime polar ozone depletion in the CMAM run without heterogeneous chemistry, the seasonal cycle shows a late spring maximum in polar regions and hence a strong seasonal cycle (in fact approaching that of the NH; see below) in the entire extratropical region. However, the persistence of ozone anomalies and the photochemical decay is very similar to that in the observations as well as in the other CMAM run (Fig. 4). This shows that this diagnostic reflects transport and summertime photochemistry, and does not depend on how the springtime ozone anomaly is created.

We now examine the behaviour in the NH. Figure 6 shows the seasonal cycle of total ozone over 35° N–60° N, 60° N–80° N, and 35° N–80° N for the observations and the CMAM (with heterogeneous chemistry). As before, the observed values are the anomalies from the long term trend added to the EESC fit for the year 2000. The seasonal cycles are in good agreement, but CMAM has comparatively limited interannual variability in midlatitudes and thus over 35° N–80° N as a whole. This deficiency is evident in other CMAM diagnostics (Austin et al., 2003), and may reflect the fact that CMAM has been run with fixed external forcings and annually repeating sea surface temperatures. (Also, this version of CMAM does not exhibit a quasi-biennial oscillation.)

In the observations, F&S 2003 showed that interannual anomalies in NH midlatitudes persist through summer, despite the mixing in of polar air following the vortex breakdown. This is because in terms of total ozone mass, the midlatitude anomalies dominate over the polar anomalies; the anomalies seen in Fig. 6 are multiplied by the area of the region. (This is also why the seasonal variation in midlatitude ozone trends

in the NH is largely unaffected by the polar trends (F&S 2005).) However in CMAM the midlatitude anomalies decay rapidly after the vortex breakdown, because of the relatively large impact, compared to observations, of the CMAM polar anomalies. For the entire 35° N–80° N region the CMAM anomalies, although small in magnitude, are persistent. The decay of the anomalies is shown in Fig. 7 and is virtually identical between CMAM and the observations. (The high value of the correlations is reflected in the small error bars for the regression coefficients.)

4 Summary

The persistence and photochemical decay of springtime total ozone anomalies in CMAM over 35°–80° latitude in both hemispheres is very realistic. The behaviour in the SH is similar for simulations with and without heterogeneous chemistry, i.e. with or without an ozone hole. The behaviour in the NH is realistic despite unrealistically low ozone variability. This shows that the diagnostic from F&S 2003 does not depend on how the springtime anomalies are created or on their magnitude, but reflects the transport and photochemical decay in the model. It is thus a robust, process-oriented diagnostic of model performance.

Acknowledgements. This work has been supported by the GCC project, with funding from the Natural Sciences and Engineering Research Council of Canada, the Canadian Foundation for Climate and Atmospheric Sciences, the Canadian Space Agency, and Environment Canada. The authors are indebted to J. de Grandpré for assistance with the CMAM data set, to V. Fioletov for helpful discussions, and to R. Stolarski and S. Frith from NASA for making the merged satellite data set available. Work at AWI was supported by the EC under contract 505390-GOCE-CT-2004 (SCOUT-O3).

References

Austin, J., Shindell, D., Beagley, S. R., Brühl, C., Dameris, M., Manzini, E., Nagashima, T., Newman, P., Pawson, S., Pitari, G., Rozanov, E., Schnadt, C., and Shepherd, T. G.: Uncertainties and assessments of chemistry-climate models of the stratosphere, Atmos. Chem. Phys., 3, 1–27, 2003.

Beagley, S. R., de Grandpré, J., Koshyk, J. N., McFarlane, N. A., and Shepherd, T. G.: Radiative-dynamical climatology of the first-generation Canadian Middle Atmosphere Model, Atmos.-Ocean, 35, 293–331, 1997.

de Grandpré, J., Beagley, S. R., Fomichev, V. I., Griffioen, E., McConnell, J. C., Medvedev, A. S., and Shepherd, T. G.: Ozone climatology using interactive chemistry: results from the Canadian Middle Atmosphere Model, J. Geophys. Res., 105, 26 475–26 491, 2000.

Fioletov, V. E., Bodeker, G. E., Miller, A. J., McPeters, R. D., and Stolarski, R.: Global and zonal total ozone variations estimated from ground-based and satellite measurements: 1964–2000, J. Geophys. Res., 107, 4647, doi:10.1029/2001JD001350, 2002.

Fioletov, V. E. and Shepherd, T. G.: Seasonal persistence of midlatitude total ozone anomalies, Geophys. Res. Lett., 30, 1417, doi:10.1029/2002GL016739, 2003.

Fioletov, V. E. and Shepherd, T. G.: Summertime total ozone variations over middle and polar latitudes, Geophys. Res. Lett., 32, L04807, doi:10.1029/2004GL022080, 2005.

Frith, S., Stolarski, R., and Bhartia, P. K.: Implications of version 8 TOMS and SBUV data for long-term trend analysis, Proceedings of the Quadrennial Ozone Symposium-2004, edited by: Zerefos, C., 65–66, 2004.

Weber, M., Dhomse, S., Wittrock, F., Richter, A., Sinnhuber, B. M., and Burrows, J. P.: Dynamical control of NH and SH winter/spring total ozone from GOME observations in 1995–2002, Geophys. Res. Lett., 30, 1583, 2003.

WMO: Scientific Assessment of Ozone Depletion: 2002, World Meteorological Organisation Global Ozone Research and Monitoring Project Report No. 47, Geneva, 2003.

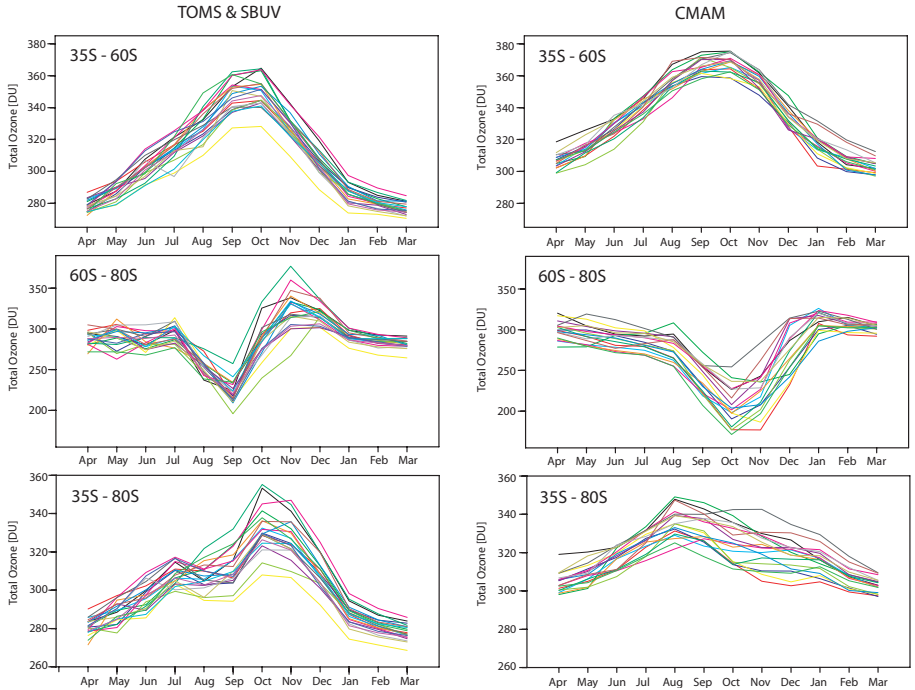

Fig. 1. Seasonal cycle of area weighted total ozone values averaged over SH midlatitudes (35° S–60° S), polar latitudes (60° S–80° S), and the entire extratropical region (35° S–80° S), for the merged TOMS & SBUV data set on the left hand side and for CMAM on the right hand side. Each curve corresponds to a different year. The observed values are the anomalies from the long term trend added to the EESC fit for the year 2000.

ACPD
6, 3403–3417, 2006

S. Tegtmeier and T. G. Shepherd

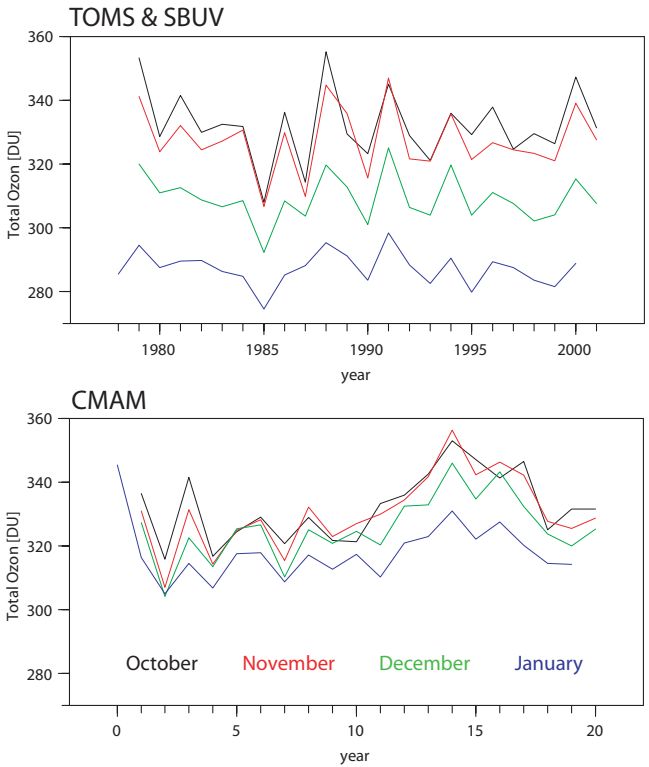

Fig. 2. Time series of total ozone averaged over 35° S–80° S for the four spring/early summer months for the observations (normalized to the year 2000) and for CMAM.

ACPD
6, 3403–3417, 2006

EGU

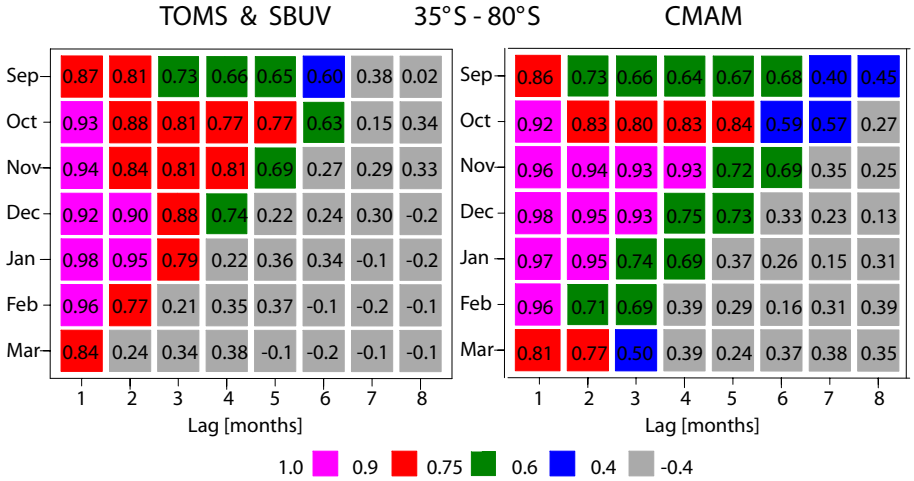

Fig. 3. Correlation coefficients between ozone anomalies at a given month of the year with ozone anomalies at subsequent months for 35° S–80° S, for the observations and for CMAM. Values shaded gray are not statistically significant at the 95% level.

ACPD
6, 3403–3417, 2006

S. Tegtmeier and T. G. Shepherd

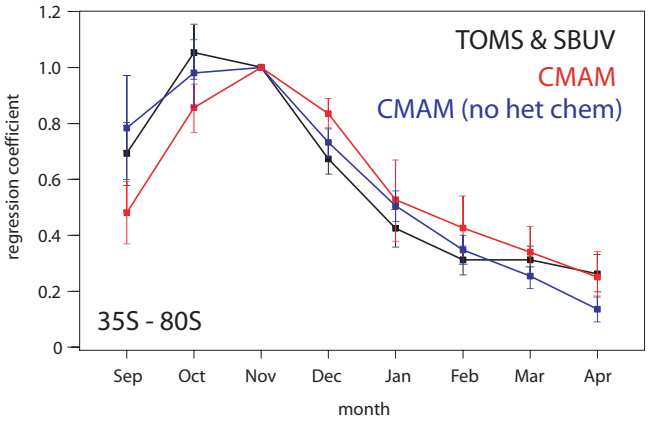

Fig. 4. Linear regression coefficients between 35° S–80° S ozone anomalies in November and in other months of the year for the observations (black line), the CMAM run with heterogeneous chemistry (red line), and a CMAM run without heterogeneous chemistry (blue line). The error bars indicate the 1σ uncertainty.

ACPD
6, 3403–3417, 2006

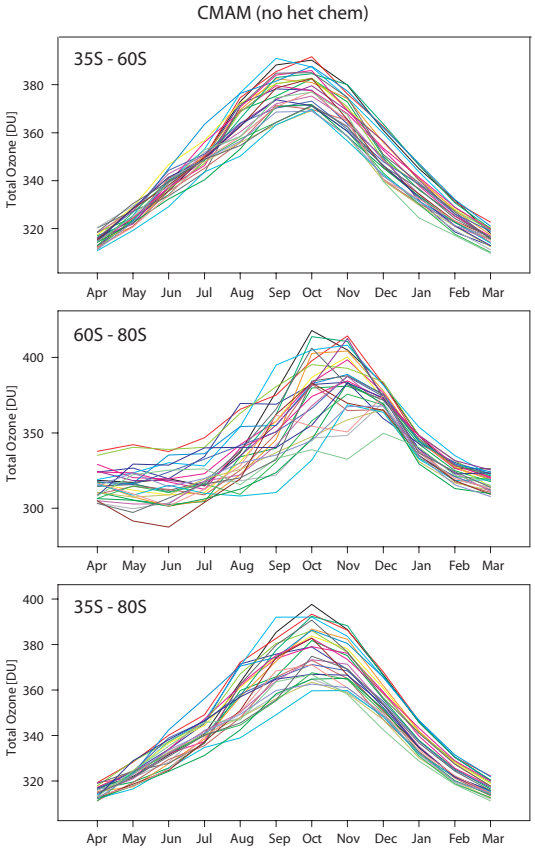

Fig. 5. As in Fig. 1, but for the CMAM run without heterogeneous chemistry.

ACPD
6, 3403–3417, 2006

EGU

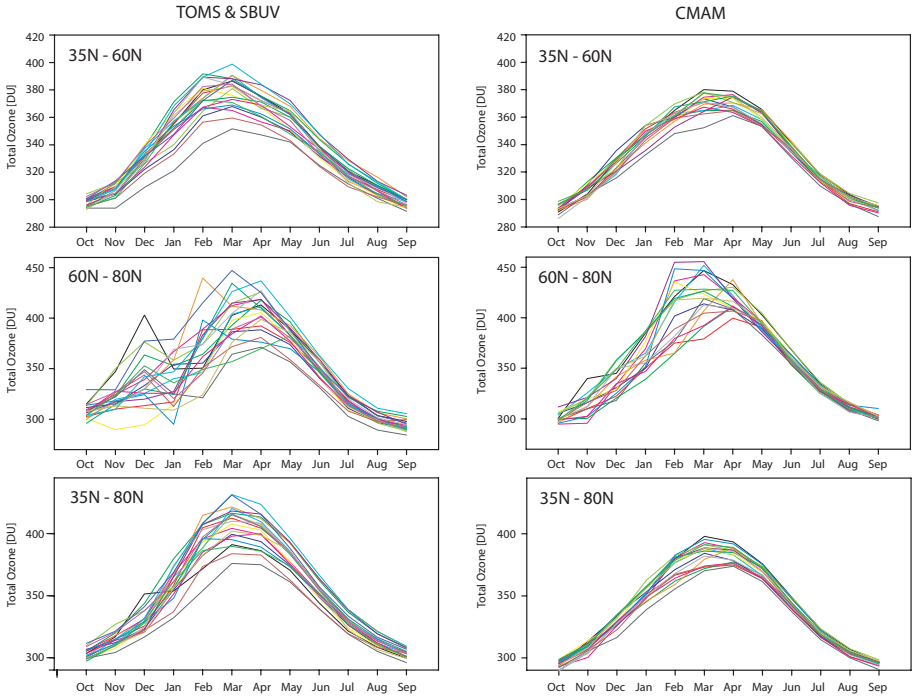

Fig. 6. As in Fig. 1, but for the NH.

ACPD
6, 3403–3417, 2006

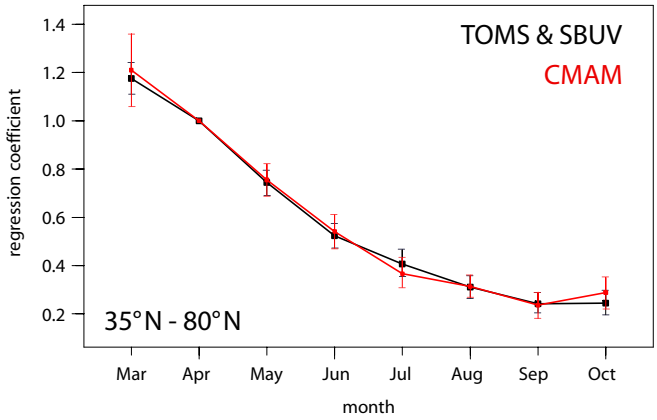

Fig. 7. Linear regression coefficients between 35° N–80° N ozone anomalies in April and in other months of the year for observations (black line) and the CMAM run with heterogeneous chemistry (red line). The error bars indicate the 1σ uncertainty.

ACPD
6, 3403–3417, 2006